SPATIAL CLUSTERS OF SLAB STABILITY AND SNOWPACK PROPERTIES WITHIN AVALANCHE START ZONES

Cam Campbell [1,*] and Bruce Jamieson [1,2]
[1] Department of Civil Engineering, [2] Department of Geology and Geophysics
University of Calgary, Calgary, Alberta, T2N 1N4, Canada

ABSTRACT: During the winters of 2000-01 and 2001-02, 36 spatial arrays of closely spaced small-column-type stability tests were performed, each in a day. Each array consisted of 16 to 120, 30 cm by 30 cm test columns arranged in a regular grid pattern, separated by 30 cm in both the up-slope and cross-slope directions. The point stability, slab thickness and total snowpack depth data were analyzed with a new spatial clustering technique. Thirty-three percent of the arrays showed significant spatial clusters in either high or low point stability or both, which ranged in length 1.7 m to 3.8 m. Spatial clusters of high or low slab thickness, or both, were identified in 53% of the arrays, ranging in length from 1.7 m to 3.2 m. Spatial clusters in either high or low total snowpack depth were identified in 33% of the arrays, which ranged in length from 1.8 m to 2.7 m. These lengths are the maximum dimension of the clusters and, due to the extent of the arrays, considered to be minima.

KEYWORDS: spatial variability, snow stability, avalanche start zones, clustering, snowpack stratigraphy, avalanche forecasting

1. INTRODUCTION

This study focuses on the slope-scale spatial variability of snowpack properties and slab stability with respect to point stability using dynamic loading. Spatial scale refers to the characteristic length of a process (e.g. snowpack property), measurement or model (Blöschl and Sivapalan, 1995; Hägeli and McClung, 2001). While the length scale of a process depends on the natural characteristics, the scale characteristics of measurements and models are a function of their design. Relevant scales for a study of spatial variability within avalanche start zones with respect to skier-triggering include the *snowpack-scale* (10 cm to 5 m), the *study plot-scale* (5 m to 30 m) and the *slope-scale* (5 m to 100 m). Snowpack properties and stability can vary substantially at the snowpack-scale (Jamieson, 1995, p. 65-71), the study plot-scale (Landry et al., 2004) and at the slope-scale (Campbell, 2004; Kronholm, 2004; Stewart, 2002). However, if stability tests sample all of a slope, the results are in fact variable but not random (Jamieson, 1995), which implies potential for spatial structure.

Blöschl (1999) and Hägeli and McClung (2001) identify three scale attributes of measurements (*support*, *spacing* and *extent*) dubbed the scale triplet. Support is the area or volume integrated into a single measurement, spacing is the distance between measurements, and extent is the distance spanned by a set of measurements. In order to measure the distribution of snowpack properties accurately, extent, support and spacing have to be chosen according to the natural scale characteristics of the phenomenon (Hägeli and McClung, 2001). For example, if the extent is smaller than the characteristic length of the process then the distributions appear as trends in the data (i.e. only part of the process is captured). If the extent is much larger than the characteristic length, but the support and spacing are insufficient, then the distributions appear as noise.

Campbell and Jamieson (in press) state that the slope-scale variability in snowpack properties and stability is due to a combination of various processes that act on the snowpack with various correlation lengths (ξ). Causal processes are influenced by factors such as buried rocks (assumed ξ approx. 1 m to 5 m), wind drifting (assumed ξ approx. 2 m to 10 m), slope angle (assumed ξ approx. 2 m to > 50 m) and surface hoar formation (assumed ξ approx. 1 m to > 50 m). Not only are these lengths paramount for measurement scale (support, spacing and extent) design, they can also influence the scale of stability, including point stability.

Using the same data as this study, Stewart (2002) identified 9 of 39 (23%) drop hammer arrays as having spatial clusters (i.e. groups of proximate tests) of high stability, low stability or both. Using the drop height that caused column fracture (DH) as an index of point stability, spatial cluster boundaries were defined as being straight for at least 3 adjacent tests, where:

* *Corresponding author address:* Cam Campbell, 3833 W. 12 Ave., Vancouver, B.C., Canada, V6R 2N9. Phone: 604 224 1273.
Email: cam_cam@telus.net

1. the average DH of any three tests on one side of a straight section was ten or more centimeters different than the average DH of the three closest tests on the other side;
2. and the average DH for the three tests inside a corner was ten or more centimeters different than the average DH of the four tests outside a corner.

Stewart (2002) also showed that eight of the arrays had significant positive and eight arrays had significant negative Spearman rank correlations between DH and slab thickness (*H*). While a positive relationship (i.e. greater stability for thicker slabs) between stability (DH) and *H* is supported by slab mechanics (i.e. the stress from a skier decreases as *H* increases) and results from Campbell and Jamieson (in press), a negative relationship is difficult to explain. Stewart (2002, p. 59-60) hypothesized that the explanation involved the difference between a stress wave traveling through a test column with a confined cross section and a skier's unconfined stress pattern. While a skier's stress spreads laterally and rapidly diminishes in magnitude with increasing depth (Schweizer and Camponovo, 2001), a stress wave traveling through a confined column is less likely to do so. This may explain why Campbell and Jamieson (in press) were able to detect predominately positive effects of *H* on stability with the rutschblock test, which has a cross-section large enough to incorporate a skiers stress pattern.

The objectives of this study are:

1. to try a new method for identifying spatial clusters in arrays for which variogram modeling did not reveal a range, probably due the limited extent and sample size of the arrays, and
2. to use these clusters to identify possible causes of spatial variability in arrays for which correlation analysis did not reveal conclusive effects, again probably due to insufficient extent and sample size.

2. METHODS

2.1 Research area

Field research for this study was carried out by graduate students and research technicians based out of two separate field stations in the Columbia Mountains of British Columbia (Figure 1). The Rogers Pass field station is located in Glacier National Park, with many arrays on Mt. Fidelity. The Blue River field station is located in the Cariboo and Monashee Mountains with some arrays on Mt. St. Anne. Arrays were also performed in the Purcell Mountains about 10 km west of Golden near the Kicking Horse Mountain Resort.

The Columbia Mountains are characterized by a transitional climate with a heavy maritime influence. The snowpack at treeline is usually deeper than 2 m throughout the winter and often includes persistent weak layers of buried surface hoar or faceted crystals (Hägeli and McClung, 2003).

Whenever possible field research was carried out in avalanche start zones; however, if avalanche danger compromised worker safety, sites with variability characteristic of avalanche start zones were used.

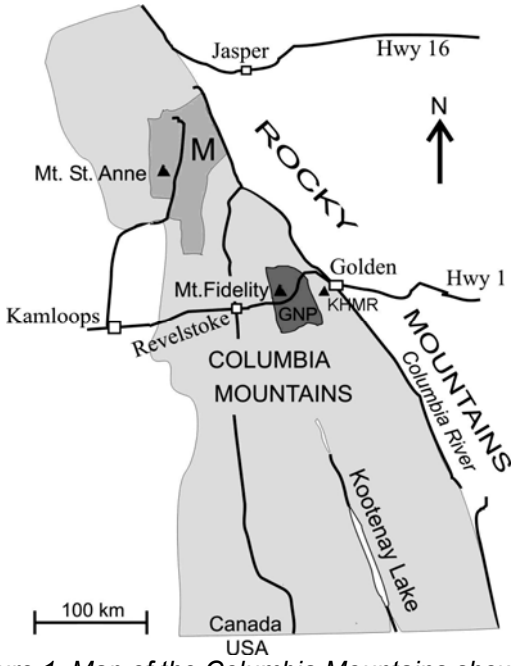

Figure 1. Map of the Columbia Mountains showing the Blue River study area around Mt. St. Anne (M) and Glacier National Park (GNP) where the Rogers Pass field station is located. The third study area is in the Purcells near the Kicking Horse Mountain Resort (KHMR).

2.2 Field methods

A small-column-type stability test was used to estimate slab stability. The 30 cm x 30 cm test columns were arranged in a regular grid pattern separated by 30 cm in both the up-slope and cross-slope directions. During the winters of 2000-01 and 2001-02, 39 spatial arrays were performed, ranging in size from 16 to 120 tests (Stewart, 2002). Three of these arrays were not used in this study due to insufficient data.

Similar to the rammrutsch device (Schweizer et al., 1995), a drop hammer device (Figure 2) was used to load the columns. An appropriate hammer mass (1 kg or 3 kg) was chosen based on practice test results then mounted on the graduated guide rod. The hammer was dropped from successive 5 cm height increments, starting from 5 cm, until the fracture propagated along a weak snowpack layer across the entire test column. The drop height (cm) which causes the fracture to propagate (DH) was then recorded. If the fracture propagated when the device was gently placed on the column, before the hammer was dropped, a DH of 0.1 cm was assigned to that test. If the fracture did not propagate after the end of the guide rod was reached (60 cm) then a DH of 70 cm was assigned to that test.

The drop hammer test is used as an index of point stability because Stewart (2002) found a strong linear correlation between the results of drop hammer tests and adjacent compression tests (Greene et al., 2004, p. 45-47; Canadian Avalanche Association, 2002, p. 33-34), the latter of which is a commonly used test of point stability.

Total snowpack depth (HS) and slab thickness (*H*) were also measured for every test using a graduated probe pole or ruler, respectively.

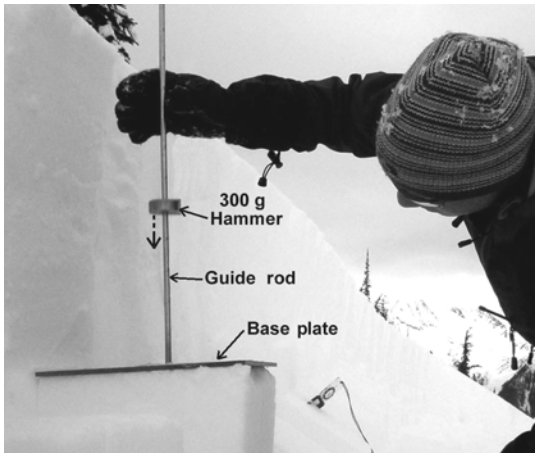

Figure 2. The drop hammer device with a base plate, graduated guide rod and hammer being used to load a test column.

2.3 Statistical methods

The spatial clusters were identified first by identifying numerical clusters, independent of position within arrays, and then assessing if the data in the numerical clusters were grouped spatially.

Numerical clusters were identified with the k-means clustering technique, which uses analysis of variance (ANOVA) calculations to determine an F-statistic (i.e. ratio of the variability between clusters to the variability within clusters). The number of clusters (*k*) was chosen to maximize F. ANOVA assumes that the clusters are normally distributed and have equal variances; however, Stewart (2002) showed that the data violated these assumptions. Therefore, numerical clusters were verified using the non-parametric Kruskal-Wallis and Mann-Whitney U tests to a significance level of 0.05. This means that there is less than a five percent chance of considering the clusters to be significantly different when, in fact, they are not (Type 1 error).

Stewart (2002, p. 80) plotted variograms of test results for all 36 arrays. Variograms are graphs of the difference in DH quantified by the semi-variance versus the distance between two tests or lag distance. DH for all 36 arrays but three (the arrays performed on 28 February 2001, 6 April 2001 and 23 November 2001) showed increasing semi-variance with lag distance, for lag distances less than 1.2 m. This suggests that spatial autocorrelation exists for adjacent tests. However, the extent of the arrays was insufficient to determine correlation lengths with the variograms.

The Kruskal-Wallis test statistic (H_{KW}) is essentially the average of the squared deviations of the cluster mean ranks from the average total rank with *k* minus one degrees of freedom, where greater values of H_{KW} correspond to greater differences between clusters. The Kruskal-Wallis test is, however, only valid for three or more clusters; therefore, the Mann-Whitney U test was used to test independence in situations where $k = 2$. The Mann-Whitney U test determines the significance of differences in average ranks for two clusters. For sample sizes greater than 20, the Mann-Whitney *U*-statistic approaches a normal distribution. It is therefore common to use the parametric *z*-value (i.e. larger absolute *z*-values correspond with greater differences in average cluster ranks) in combination with a p-value to express significance. However, both the Kruskal-Wallis and the Mann-Whitney U test assume that the samples are independent and the variograms suggested otherwise because of spatial autocorrelation between stability tests. P-values are therefore not good measures of Type 1 errors for these arrays.

Spatial clusters were selected that were likely indicative of physical processes. We defined a unique spatial cluster as one that had at least four

adjacent tests (imposing a minimum length), which belonged to the numerical cluster with either the highest or lowest average DH for the array and was bounded by either an array boundary or by tests belonging to another numerical cluster. In addition, the cluster boundaries had no more than ten corners because we consider such clusters to be less indicative of a continuous physical process. Figure 3 shows examples of clusters that were rejected because they failed to meet these criteria.

One disadvantage of the method is that spatial clusters are partly identified by numerical clusters that can include values outside the spatial cluster.

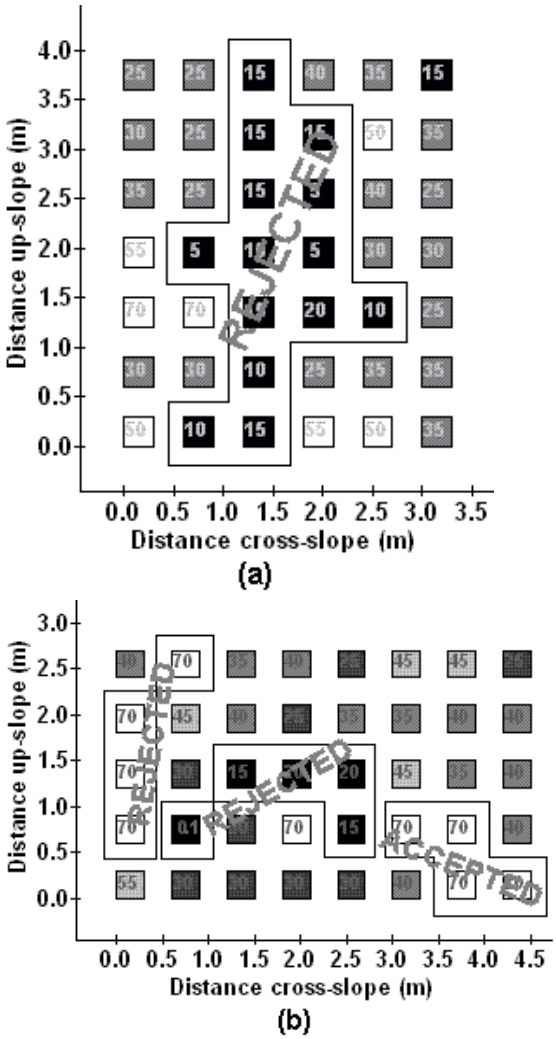

Figure 3. Examples of numerical clusters that were rejected as spatial clusters because they did not meet the specified criteria. Each square represents a test column shaded according to the numerical cluster to which it belongs, where black represents the numerical cluster with the lowest average DH and white represents the numerical cluster with the highest average DH for the array. Drop heights (cm) are also indicated. The array shown in example (a) (performed on 4 January 2002)) has a cluster of low DH that was rejected because the boundary has more than ten corners. The array shown in example (b) (performed on 25 January 2001) has a cluster of high DH on the right side that met the criteria; however, the cluster of low DH in the middle of the array was rejected because the bottom left corner is not bounded entirely by tests belonging to another numerical cluster.

The use of array boundaries as cluster boundaries, when we cannot guarantee cluster isolation, can be justified in several ways. First of all, the criterion of a unique spatial cluster encompassing at least four tests reduces the likelihood of identifying a spatial cluster when in fact there is no spatial structure whatsoever. Second, due primarily to time constraints while ensuring temporal variability was minimized, the extent of the arrays was often sufficient to capture only one cluster. The lengths of the clusters were therefore considered to be minima and no attempt was made to define maximum lengths.

H and HS were also clustered in this manner. Cluster lengths can provide an estimate of the correlation lengths and hence the process scales associated with these snowpack properties. However, relating variable stability within avalanche start zones to causal processes can be difficult with current methods (Kronholm, 2004) due to the measurement and temporal scales of current field tests.

Stewart (2002, p. 68) found no significant correlations between DH and sequence number (i.e. relative time at which each test in an array was performed) and therefore concluded that the test scores within arrays did not exhibit temporal variability.

3. RESULTS

Figure 4 shows the distribution of DH (cm) for all 36 arrays. Note that because two different hammers (1 kg or 3 kg) were used, the variability and magnitude of DH from one array cannot be compared to another. Twenty-three arrays had persistent weak layers, including buried surface hoar (17 arrays) and faceted crystals (6 arrays), as the primary failure layer. Thirteen arrays had non-persistent weak layers, including decomposed and fragmented crystals (8 arrays), melt-freeze crusts (3 arrays) and rounded grains (2 arrays), as the

primary failure layer (Stewart, 2002). However, it is likely that there were faceted crystals associated with these melt-freeze crusts (Jamieson, 2006) but the facet layers may have been too thin to reliably observe.

Table 1 lists both the numerical and spatial clustering results for DH. All but one (performed on 27 February 2002) of the 36 arrays had significant numerical clusters in DH, with *k* ranging from 2 to 7. Twelve (33%) of the 36 arrays had spatial clusters of high DH, low DH or both. The maximum dimension (*l*) of the clusters ranged from 1.7 m to 3.8 m, but this is often constrained by array boundaries. The *l* is measured either up-slope, cross-slope or diagonally, whichever is greatest, within the confines of the cluster boundary based on each tests encompassing a 60 cm by 60 cm area (i.e. in addition to the area of the test column each test represents 15 cm on all sides in both the up-slope and cross-slope directions). Neither the number nor the size of high DH clusters differed significantly from the number or size of low DH clusters. This suggests that encountering an area of relatively high stability is just as likely as encountering an area of relatively low stability, which is in contrast to early ideas in spatial variability of stability. Munter (1991, p. 111) opines that zones of high stability surrounded by low stability is more likely.

The clustering methods used for this study approximately agreed with Stewart's (2002) clusters in two arrays: 14 December 2001 (one of three clusters) and 7 February 2001, but not for seven other of Stewart's (2002) arrays with clusters.

Table 2 lists both the numerical clustering and the spatial clustering results for *H*. All of the 36 arrays had significant numerical clusters in *H*, with *k* ranging from 2 to 14. Nineteen (53%) of the 36 arrays had spatial clusters of high *H*, low *H* or both. The *l* of the clusters ranged from 1.7 m to 3.2 m, roughly the same size as the spatial clusters in DH. Even though this shows that the processes that affect stability and *H* could have similar process scales and hence, *H* could be a predictor of variations in stability, only three arrays had spatial clusters of *H* in the same area as DH, and two showed a positive relationship while one showed a negative relationship. Neither the number nor the size of high *H* clusters differed significantly from the number or size of low *H* clusters. This suggests that encountering an area of relatively high slab thickness is just as likely as encountering an area of relatively low slab thickness.

Table 3 lists both the numerical clustering and the spatial clustering results for HS. All of the 36 arrays had significant numerical clusters in HS, with *k* ranging from 4 to 15. Twelve (33%) of the 36 arrays had spatial clusters of high HS or low HS. The *l* of the clusters ranged from 1.8 m to 2.7 m, somewhat lower than the range of *l* for DH and *H*. The number of clusters of low HS (8) was somewhat higher than the number of clusters of high HS (5). This is to be expected because the processes that cause variations in HS (e.g. buried boulders, logs and stumps) will only cause spatial clusters of low HS.

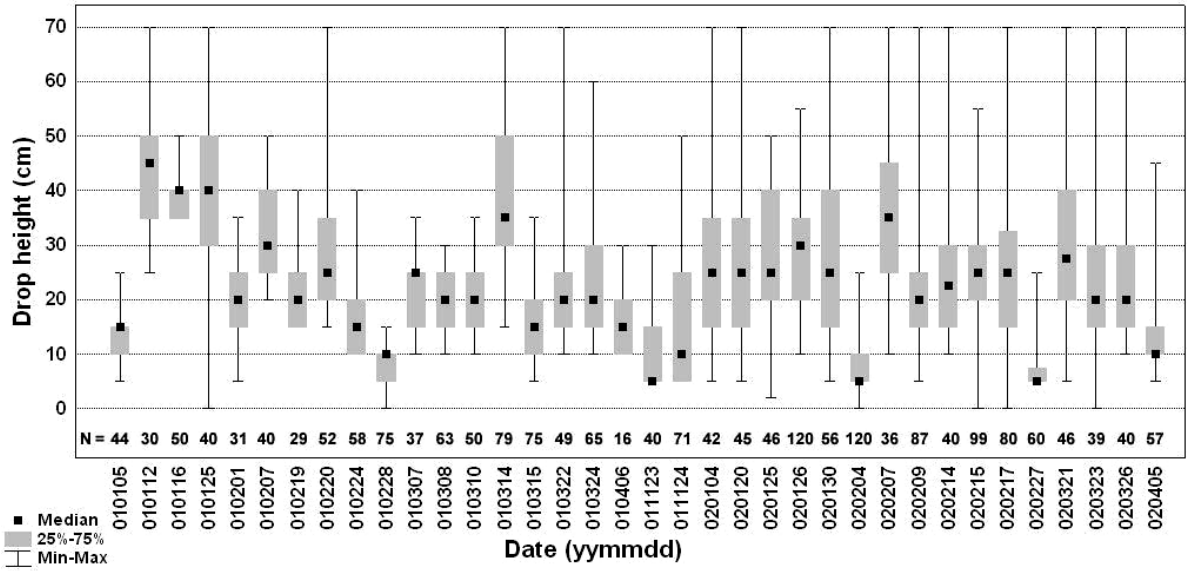

Figure 4. Box plots of the drop height (cm) distribution for all 36 drop hammer arrays listed according to array date (yymmdd)*. The number of tests (N), median, inter-quartile range and range are shown.*

Table 1. Clustering results for drop height (DH) for all 36 drop hammer arrays listed according to array date (yymmdd). *Numerical clustering results including the number of clusters (k), the Kruskal-Wallis statistic (H_{KW}) and significance (ρ) for k ≥ 3 and the z-statistic (z) and Mann-Whitney significance (ρ) for k = 2 are shown. Spatial clustering results for clusters of high and low drop height (DH), including the number of tests (n) and the maximum dimension (l), are also shown. Respective results for more than one cluster per array are separated by a comma.*

Date (yymmdd)	Numerical clusters					Spatial clusters			
	k	Kruskal-Wallis		Mann-Whitney		High DH		Low DH	
		H_{KW}	ρ	z	ρ	n	l (m)	n	l (m)
010105	2	~	~	5.92	$< 10^{-3}$	~	~	~	~
010112	4	27.3	$< 10^{-3}$	~	~	~	~	~	~
010116	2	~	~	6.01	$< 10^{-3}$	~	~	6	2.7
010125	5	37.9	$< 10^{-3}$	~	~	4	2.2	~	~
010201	3	26.4	$< 10^{-3}$	~	~	4	2.2	~	~
010207	5	38.1	$< 10^{-3}$	~	~	8, 4	3.0, 2.2	~	~
010219	2	~	~	-4.32	$< 10^{-3}$	~	~	~	~
010220	5	49.7	$< 10^{-3}$	~	~	~	~	~	~
010224	2	~	~	6.52	$< 10^{-3}$	~	~	~	~
010228	2	~	~	-8.15	$< 10^{-3}$	~	~	~	~
010307	3	30.8	$< 10^{-3}$	~	~	~	~	10	3.5
010308	2	~	~	-6.32	$< 10^{-3}$	~	~	~	~
010310	4	46.9	$< 10^{-3}$	~	~	~	~	~	~
010314	4	73.4	$< 10^{-3}$	~	~	~	~	~	~
010315	3	68.9	$< 10^{-3}$	~	~	~	~	~	~
010322	3	36.4	$< 10^{-3}$	~	~	~	~	7	2.7
010324	3	47.2	$< 10^{-3}$	~	~	~	~	~	~
010406	2	~	~	3.26	0.001	~	~	11	3.8
011123	2	~	~	5.45	$< 10^{-3}$	~	~	~	~
011214	2	~	~	-6.92	$< 10^{-3}$	4	2.4	~	~
020104	3	35.1	$< 10^{-3}$	~	~	~	~	~	~
020120	3	36.8	$< 10^{-3}$	~	~	5	2.4	7	3.0
020125	7	44.2	$< 10^{-3}$	~	~	~	~	~	~
020126	3	105.6	$< 10^{-3}$	~	~	~	~	~	~
020130	2	~	~	-6.21	$< 10^{-3}$	~	~	~	~
020204	2	~	~	10.1	$< 10^{-3}$	~	~	~	~
020207	5	32.3	$< 10^{-3}$	~	~	~	~	4	2.2
020209	3	68.2	$< 10^{-3}$	~	~	~	~	~	~
020214	3	31.7	$< 10^{-3}$	~	~	~	~	~	~
020215	4	90.6	$< 10^{-3}$	~	~	6, 4	3.6, 1.7	8	3.0
020217	4	74.1	$< 10^{-3}$	~	~	~	~	~	~
020227	0	~	~	~	~	~	~	~	~
020321	5	41.6	$< 10^{-3}$	~	~	~	~	~	~
020323	5	36.2	$< 10^{-3}$	~	~	~	~	~	~
020326	3	29.0	$< 10^{-3}$	~	~	~	~	~	~
020405	2	~	~	-6.39	$< 10^{-3}$	7	3.2	6	3.0

Table 2. Clustering results for slab thickness (H) for all 36 drop hammer arrays listed according to array date (yymmdd). *Numerical clustering results including the number of clusters (k), the Kruskal-Wallis statistic (H_{KW}) and significance (ρ) for k ≥ 3 and the z-statistic (z) and Mann-Whitney significance (ρ) for k = 2 are shown. Spatial clustering results for clusters of high and low slab thickness (H), including the number of tests (n) and the maximum dimension (l), are also shown. Respective results for more than one cluster are separated by a comma.*

Date (yymmdd)	Numerical clusters					Spatial clusters			
	k	Kruskal-Wallis		Mann-Whitney		High H		Low H	
		H_{KW}	ρ	z	ρ	n	l	n	l
010105	5	41.5	$< 10^{-3}$	~	~	6	3.0	5	2.7

010112	3	21.7	$< 10^{-3}$	~	~	8	3.2	~	~
010116	2	~	~	-6.32	$< 10^{-3}$	~	~	~	~
010125	4	35.2	$< 10^{-3}$	~	~	~	~	~	~
010201	7	30.3	$< 10^{-3}$	~	~	5	2.7	~	~
010207	4	36.4	$< 10^{-3}$	~	~	5	2.7	5	2.2
010219	3	22.6	$< 10^{-3}$	~	~	~	~	~	~
010220	4	46.4	$< 10^{-3}$	~	~	~	~	7	2.5
010224	5	54.6	$< 10^{-3}$	~	~	~	~	6	3.2
010228	2	~	~	7.70	$< 10^{-3}$	~	~	~	~
010307	2	~	~	-5.36	$< 10^{-3}$	~	~	5	2.2
010308	3	56.7	$< 10^{-3}$			7	2.5	8, 6	3.0, 2.2
010310	2	~	~	5.75	$< 10^{-3}$	~	~	~	~
010314	7	76.3	$< 10^{-3}$	~	~	~	~	~	~
010315	2	~	~	7.39	$< 10^{-3}$	~	~	~	~
010322	7	46.2	$< 10^{-3}$	~	~	~	~	~	~
010324	6	61.2	$< 10^{-3}$	~	~	~	~	~	~
010406	3	13.4	0.001	~	~	6	2.2	4	2.2
011123	3	31.2	$< 10^{-3}$	~	~	~	~	~	~
011214	11	70.6	$< 10^{-3}$	~	~	~	~	~	~
020104	14	40.8	$< 10^{-3}$	~	~	~	~	4	2.2
020120	6	42.6	$< 10^{-3}$	~	~	4	2.2	~	~
020125	6	44.1	$< 10^{-3}$	~	~	~	~	~	~
020126	7	116.2	$< 10^{-3}$	~	~	4	1.7	6	2.4
020130	8	53.9	$< 10^{-3}$	~	~	~	~	~	~
020204	6	118.6	$< 10^{-3}$	~	~	~	~	~	~
020207	7	33.2	$< 10^{-3}$	~	~	~	~	4	2.4
020209	8	84.6	$< 10^{-3}$	~	~	~	~	8	3.0
020214	10	38.5	$< 10^{-3}$	~	~	4	2.2	~	~
020215	7	95.3	$< 10^{-3}$	~	~	~	~	5	2.2
020217	6	85.4	$< 10^{-3}$	~	~	~	~	~	~
020227	3	53.6	$< 10^{-3}$	~	~	~	~	~	~
020321	4	38.2	$< 10^{-3}$	~	~	~	~	5	3.0
020323	4	33.1	$< 10^{-3}$	~	~	8	2.4	~	~
020326	4	38.1	$< 10^{-3}$	~	~	4	2.4	~	~
020405	4	56.3	$< 10^{-3}$	~	~	~	~	~	~

Table 3. Clustering results for total snowpack depth (HS) for all 36 drop hammer arrays listed according to array date (yymmdd)*. Numerical clustering results including the number of clusters (k), the Kruskal-Wallis statistic (H_{KW}) and significance (ρ) for k ≥ 3 and the z-statistic (z) and Mann-Whitney significance (ρ) for k = 2 are shown. Spatial clustering results for clusters of high and low snowpack depth (HS), including the number of tests (n) and the maximum dimension (l), are also shown. Respective results for more than one cluster are separated by a comma.*

Date (yymmdd)	**Numerical clusters**					**Spatial clusters**			
		Kruskal-Wallis		**Mann-Whitney**		**High HS**		**Low HS**	
	k	H_{KW}	**ρ**	***z***	**ρ**	***n***	***l***	***n***	***l***
010105	15	43.8	$< 10^{-3}$	~	~	~	~	4, 4	2.2, 1.8
010112	15	28.9	0.011	~	~	~	~	5	2.5
010116	7	48.2	$< 10^{-3}$	~	~	~	~	4	2.2
010125	5	36.6	$< 10^{-3}$	~	~	~	~	~	~
010201	14	30.8	0.004	~	~	~	~	5	2.2
010207	13	38.8	$< 10^{-3}$	~	~	~	~	4	2.2
010219	9	28.5	$< 10^{-3}$	~	~	~	~	~	~
010220	10	52.4	$< 10^{-3}$	~	~	5	2.2	~	~
010224	5	54.8	$< 10^{-3}$	~	~	~	~	4	2.2
010228	9	72.3	$< 10^{-3}$	~	~	~	~	~	~
010307	7	38.2	$< 10^{-3}$	~	~	~	~	~	~

010308	10	62.3	$< 10^{-3}$	~	~	~	~	~	~
010310	8	47.7	$< 10^{-3}$	~	~	~	~	~	~
010314	6	75.1	$< 10^{-3}$	~	~	7	2.7	~	~
010315	15	73.6	$< 10^{-3}$	~	~	~	~	~	~
010322	8	45.4	$< 10^{-3}$	~	~	~	~	~	~
010324	8	62.7	$< 10^{-3}$	~	~	5	2.7	~	~
010406	6	14.4	0.013	~	~	~	~	~	~
011123	11	38.6	$< 10^{-3}$	~	~	~	~	~	~
011214	9	69.7	$< 10^{-3}$	~	~	~	~	~	~
020104	7	39.9	$< 10^{-3}$	~	~	~	~	~	~
020120	9	43.9	$< 10^{-3}$	~	~	~	~	~	~
020125	10	45.0	$< 10^{-3}$	~	~	~	~	~	~
020126	8	116.5	$< 10^{-3}$	~	~	~	~	~	~
020130	10	55.4	$< 10^{-3}$	~	~	~	~	~	~
020204	8	119.6	$< 10^{-3}$	~	~	~	~	~	~
020207	9	34.5	$< 10^{-3}$	~	~	~	~	~	~
020209	8	86.1	$< 10^{-3}$	~	~	~	~	~	~
020214	7	37.6	$< 10^{-3}$	~	~	~	~	~	~
020215	8	101.0	$< 10^{-3}$	~	~	~	~	~	~
020217	7	85.1	$< 10^{-3}$	~	~	4	2.2	~	~
020227	4	55.5	$< 10^{-3}$	~	~	~	~	~	~
020321	5	44.1	$< 10^{-3}$	~	~	~	~	~	~
020323	4	35.7	$< 10^{-3}$	~	~	5	2.5	~	~
020326	5	37.0	$< 10^{-3}$	~	~	~	~	~	~
020405	9	69.9	$< 10^{-3}$	~	~	~	~	4	2.4

3.1 Example arrays

The array shown in Figure 5 was performed 7 February 2001. The primary failure layer was decomposed and fragmented crystals. Two unique spatial clusters of high DH were found for this array: one in the upper left corner with n = 8 and l = 3.0 m and one in the lower right corner with n = 4 and l = 2.2 m. The cluster in the lower right corner corresponded with a spatial cluster of high H values with n = 5 and l = 2.7 m. This suggests that the thicker slab could have resulted in higher stability.

The array shown in Figure 6 was performed 22 March 2001. The primary failure layer was indicated as a melt-freeze crust. A spatial cluster of low DH was found in the middle of the array, with n = 7 and l = 2.7. This was the only spatial cluster of DH that was not bounded on at least one side by the edge of the array.

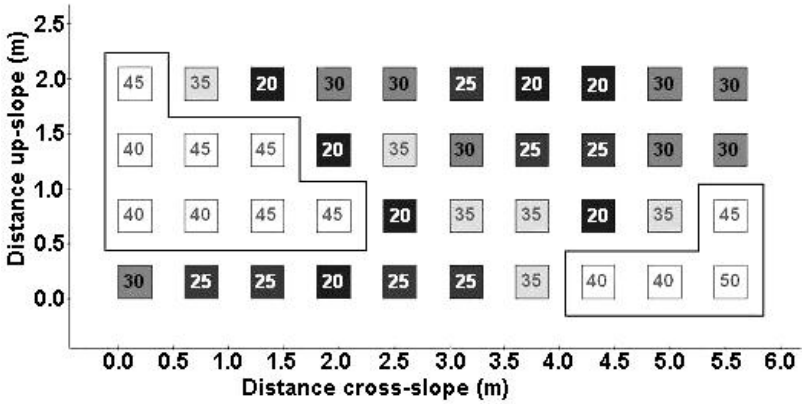

Figure 5. Drop heights (cm) for the array performed on 7 February 2001. Each square represents a test column shaded according to the numerical cluster to which it belongs, where black represents the numerical cluster with the lowest average DH and white represents the numerical cluster with the highest average DH for the array. Two clusters of high drop heights are indicated: one consisting of eight tests in the upper left corner and one consisting of four tests in the lower left corner.

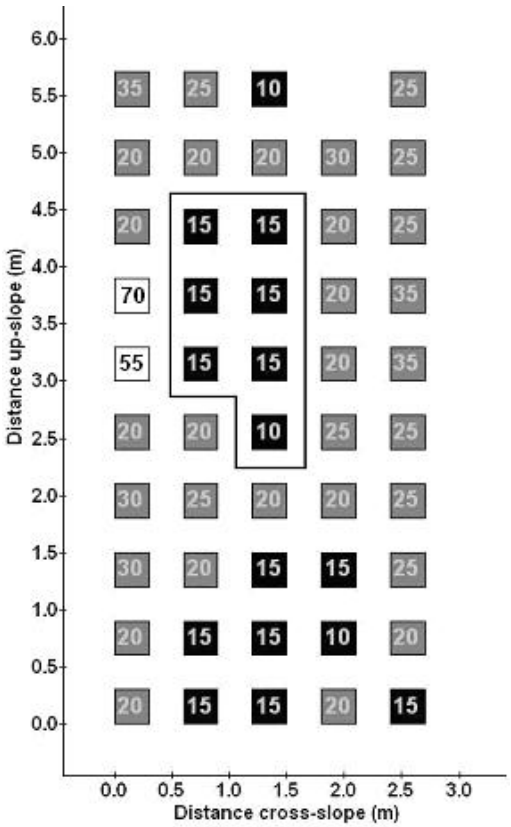

Figure 6. Drop heights (cm) for the array performed on 22 March 2001. Each square represents a test column shaded according to the numerical cluster to which it belongs, where black represents the numerical cluster with the lowest average DH and white represents the numerical cluster with the highest average DH for the array. A cluster of seven tests with low drop heights in the middle of the array is indicated.

4. CONCLUSIONS

A high level of spatial variability of point stability exists in avalanche start zones with, in most cases using current techniques, indefinable spatial structure. In this and other studies (e.g. Kronholm et al., 2004), few arrays exhibit spatial structure. Perhaps the number of data and extent were insufficient to detect the structure, or the spacing was not matched to the process scales.

Using a new technique, spatial clusters in point stability were identified in 33% of the arrays with lengths ranging from at least 1.7 m to 3.8 m. Spatial clusters in slab thickness were identified in 53% of the arrays with lengths ranging from at least 1.7 m to 3.2 m. Spatial clusters in total snowpack depth were identified in 33% of the arrays with lengths ranging from at least 1.8 m to 2.7 m. These lengths are considered to be minima due to the extent of the arrays.

Clusters in *H* did not consistently correspond with clusters in DH. Therefore, the results could not suport Campbell and Jamieson's (in press) conclusion that slab thickness can have a positive effect on stability with respect to skier triggering (rutschblock score). Perhaps there is a minimum size and extent to detect the effect of slab thickness and incline on point stability or there is a problem with the difference between the small confined column of the DH test (load area = column cross section) and the much less confined column of the rutschblock test (load area << column cross section). This implies while small column tests may be good at finding weak layers, tests with columns larger than the load area may be better for assessing stability since stress waves are less confined by column cross section. Also, fracture propagation is better represented in tests with columns larger than about 1 m^2 (Schweizer et al., in press).

A new clustering method was developed that detects clusters in arrays with a limited number of tests.

5. REFERENCES

Blöschl, G. and M. Sivapalan. 1995. Scale issues in hydrological modeling – a review. Hydrological Processes, 9(3-4), 251-290.

Blöschl, G. 1999. Scaling issues in snow hydrology. Hydrological Processes, 13(14-15), 2149-2175.

Canadian Avalanche Association. 2002. Observation guidelines and recording standards for weather, snowpack and avalanches. Canadian Avalanche Association, Revelstoke, BC, Canada, 77 pp.

Campbell, C. 2004. Spatial variability of slab stability and fracture properties in avalanche start zones. M.Sc. thesis, Dept. of Civil Engineering, University of Calgary, Calgary, Alberta, Canada, 245 pp.

Campbell, C. and B. Jamieson. In press. Spatial variability of slab stability and fracture characteristics within avalanche start zones. Cold Regions Science and Technology.

Green, E., K. Birkeland, K. Elder, G. Johnson, C. Landry, I. McCammon, M. Moore, D. Sharaf, C. Sterbenz, B. Tremper and K. Williams. 2004. Snow, weather and avalanches: observational guidelines for avalanche programs in the United States. American Avalanche Association and Forest Service

National Avalanche Center, Pagosa Springs, Colorado, USA, 136 pp.
Hägeli, P. and D. M. McClung. 2001. A new perspective on computer-aided avalanche forecasting: scale and scale issues. Proceedings of the 2000 International Snow Science Workshop, Big Sky, Montana, USA.
Hägeli, P. and D. M. McClung. 2003. Avalanche characteristics of a transitional snow climate—Columbia Mountains, British Columbia, Canada. Cold Regions Science and Technology, 37, 255– 276.
Jamieson, B. 1995. Avalanche prediction for persistent snow slabs. PhD Thesis, Dept. of Civil Engineering, University of Calgary, 275 pp.
Jamieson, B. 2006. Formation of refrozen snowpack layers and their role in slab avalanche release. Reviews of Geophysics 44, RG2001, doi:10.1029/2005RG000176.
Krajewski, S. A. and B. L. Gibbs. 2001. Understanding contouring: a practical guide to spatial estimation using a computer and variogram interpretation. Gibbs Associates, Boulder, Colorado, U.S.A., 142 pp.
Kronholm, K. 2004. Spatial variability of snow mechanical properties with regard to avalanche formation. Ph.D. Dissertation, Dept. of Geography, University of Zurich, Zurich, Switzerland, 187 pp.
Kronholm, K. and J. Schweizer. 2003. Snow stability variation on small slopes. Cold Regions Science and Technology, 37, 453-465.
Kronholm, K., M. Schneebeli and J. Schweizer. 2004. Spatial variability of micropenetration resistance in snow layers on a small slope. Annals of Glaciology, 38, 202–208.
Landry, C., K. Birkeland, K. Hansen, J. Borkowski, R. Brown and R. Aspinall. 2004. Variations in snow strength and stability on uniform slopes. Cold Regions Science and Technology, 39, 205-218.
Munter, W. 1991. Neue Lawinenkunde – Ein Leitfaden für die Praxis. Verlag des Schweizer Alpen-Clubs (SAC), Bern, Switzerland.
Schweizer, J., M. Schneebeli, M. Fierz, and P. M. B. Föhn. 1995. Snow mechanics and avalanche formation: Field experiments on the dynamic response of snow cover. Surveys of Geophysics, 16(5-6), 621-633.
Schweizer, J. and C. Camponovo. 2001. The skier's zone of influence in triggering slab avalanches. Annals of Glaciology, 32, 314-320.
Schweizer, J., I McCammon and B. Jamieson. In press. Fracture mechanics and snow slope stability evaluation. Proceedings of the 2006 International Snow Science Workshop, Telluride, Colorado, USA.
Stewart, W. K. 2002. Spatial variability of slab stability within avalanche starting zones. M.Sc. Thesis, Dept. of Geology and Geophysics, University of Calgary, Calgary, Alberta, Canada, 100 pp.

6. ACKNOWLEDGEMENTS

For field work and analysis we would like to thank Kyle Stewart. For field work we would like to thank Tom Chalmers, Michelle Gagnon, Ryan Gallagher, Alan Jones, Paul Langevin, Jenn Olsen, Ilya Storm, Alec van Herwijnen and Antonia Zeidler.

For support we are grateful to the Natural Sciences and Engineering Research Council of Canada, Helicat Canada, Canadian Avalanche Association, Mike Wiegele Helicopter Skiing, Canada West Ski Area Association, and Parks Canada.